

**SYNTHESIS AND CHARACTERIZATION OF Fe-POOR OLIVINE WITH APPLICATIONS TO LOW-FeO PLANETARY SURFACES.** K. E. Vander Kaaden<sup>1</sup>, F. M. McCubbin<sup>2</sup>, R. L. Rowland<sup>1</sup>, R. V. Morris<sup>2</sup>, J. J. Reppart<sup>1,3</sup>, A. M. Lopez<sup>4</sup>, and R. L. Klima<sup>5</sup>. <sup>1</sup>Jacobs, NASA Johnson Space Center, Mail Code XI3, Houston, TX 77058, <sup>2</sup>ARES NASA Johnson Space Center, 2101 NASA Parkway, Houston, TX 77058, <sup>3</sup>Department of Geoscience, University of Las Vegas, 4505 Maryland Parkway, Las Vegas, Nevada 89154, <sup>4</sup>Department of Earth and Atmospheric Sciences, University of Houston, Houston, TX 77204, <sup>5</sup>The Johns Hopkins University Applied Physics Laboratory, Laurel, Maryland. Corresponding Author E-mail: Kathleen.e.vanderkaaden@nasa.gov

**Introduction:** Ferromagnesian silicates like olivine display a diagnostic FeO absorption feature near 1- $\mu\text{m}$  that is caused by crystal field transitions in  $\text{Fe}^{2+}$  in the crystal structure [1]. The pure Mg endmember (i.e., forsterite) does not display a 1- $\mu\text{m}$  absorption feature due to the absence of Fe in the crystalline structure. Interestingly, very little is known about exactly how much FeO is needed before the FeO band is detected in olivine. Spectral behavior near the Mg endmember changes rapidly and is not a linear function of  $X_{\text{FeO}}$  up to the point of 1- $\mu\text{m}$  band saturation [2]. Furthermore, little is known about what concentration of FeO is needed to saturate the FeO band feature. Many planetary bodies in the Solar System that are analyzed in the ultraviolet and visible wavelengths have enough FeO in the ferromagnesian silicates such that the FeO band is detected; however, a 1- $\mu\text{m}$  absorption feature has yet to be observed on the surface of Mercury, despite the presence of wt% levels of Fe on the surface detected by X-Ray Spectroscopy [e.g., 3]. Additionally, several lithologies on the Moon, particularly in the lunar highlands, which are dominated by anorthitic plagioclase, also lack a 1- $\mu\text{m}$  absorption feature [e.g., 4]. Finally, E class asteroids (proposed parent bodies of enstatite chondrites and aubrites) also do not exhibit a 1- $\mu\text{m}$  absorption feature [e.g., 5]. Consequently, obtaining a quantitative understanding of the detection limit for a 1- $\mu\text{m}$  absorption feature could substantially improve our understanding of Mercury, and aid in our understanding of low-FeO portions of the lunar surface, as well as the mineralogy/petrology of E class asteroids. In the present study, we set out to synthesize a series of low-FeO ferromagnesian minerals to place better constraints on the spectral properties of low-FeO planetary crusts.

**Methods:** One of the primary reasons we do not have quantitative constraints on the amount of FeO required to produce a 1- $\mu\text{m}$  absorption feature in olivine is the lack of pure, well-crystallized and characterized synthetic materials of appropriate composition. Suites of synthetic minerals have proven very valuable for exploring the pure Mg-Fe olivine series [e.g., 6]. We have characterized the minerals synthesized in the present study using powder X-Ray Diffraction (XRD), Electron Probe Microanalysis (EPMA), and Visible-

Near Infrared Spectroscopy (VNIRS) at NASA's Johnson Space Center (JSC).

**Table 1.** Summary of 1-bar experimental run conditions conducted for this study.

Sample	T (°C)	Run Time (hrs)	Semi-Quant XRD Match
SC-001	----	-----	100%
F-S-002	1600	$\geq 36$	100%
F-S-003	1500	$\geq 48$	100%
CF022	1100	$\geq 48$	100%
F-T-002	1600	$\geq 16$	100%
F-T-004	1600	$\geq 16$	100%

**Starting Materials.** All starting materials consisted of some combination of reagent grade oxides (e.g., MgO,  $\text{SiO}_2$ ,  $\text{Fe}_2\text{O}_3$ ), reagent grade talc (magnesium silicate monohydrate), natural talc, and natural San Carlos olivine crystals. Starting forsterite powdered mixes were produced by mixing MgO with the respective amount of either  $\text{SiO}_2$  (F-S sample labels) or talc (F-T sample labels). After weighing, the starting materials were mixed under ethanol in either a Retsch ball mill with  $\text{ZrO}_2$  cups and  $\text{ZrO}_2$  balls, or a Fritsch Pulverisette automated mixer for 30 minutes to 2 hours.

**Experimental Methods.** For all forsterite mixes, with the exception of F-S-003, each set of starting materials were loaded into a Pt-rich crucible and placed in a Lindberg oven. The sample was heated to 1600 °C and held there for a minimum of 8 hours. The power to the furnace was then shut off and the sample was left in the furnace to cool. Once cool to the touch, the crucible was removed from the furnace and the sample was reground by hand in an Fe-free mortar and pestle. The sample was then placed back in the crucible, and this process was repeated up to 2 times. The F-S-003 mix was loaded into an  $\text{Al}_2\text{O}_3$  crucible and taken to 1500 °C over the course of ~5 hours where it was held for ~8–12 hours twice.

The fayalite (CF) component was produced by weighing out the respective amounts of  $\text{SiO}_2$  and  $\text{Fe}_2\text{O}_3$ , mixing in a hand held mortar and pestle under ethanol, then running a series of heating at 1100 °C and IW+1 in a DelTech 1-atmosphere gas mixing furnace at JSC and regrinding steps.

**XRD Analyses.** Each sample was hand ground in a mortar and pestle and analyzed via powder X-ray

diffraction in a PANalytical X'Pert Pro MPD diffractometer fitted with a cobalt X-ray source ( $\text{CoK}\alpha_1$ ,  $\lambda=1.79801$  Å) and an X'celerator ( $2.02^\circ$   $2\Theta$ ) detector. The patterns were collected in angular dispersive mode from  $4.0224$  to  $79.9784^\circ 2\Theta$  with a step size of  $0.0170^\circ$  for 20.32 seconds per step. Data analysis was completed using X'Pert High Score plus software, comparing the patterns to ICDD # 98-004-7150 forsterite or # 98-000-5628 fayalite.

**Table 2.** Summary of EPMA analyses in wt% normalized to 100% for direct comparison. bd indicates the analyses were below the detection limit.

Sample	n	SiO <sub>2</sub>	MgO	Al <sub>2</sub> O <sub>3</sub>	CaO	FeO
SC-001	15	40.28	50.42	0.02	0.08	9.20
F-S-002	16	42.07	57.85	0.01	0.01	0.06
F-S-003	15	41.96	57.76	0.24	0.04	bd
CF022	10	29.15	0.01	0.01	bd	70.82
F-T-002	15	42.91	56.62	0.07	0.02	0.38
F-T-004	15	42.36	56.25	0.72	0.10	0.57

**EPMA Analyses.** Powders from each of the experimental run products were sintered and the sintered products embedded in epoxy for analysis by EPMA. All experimental run products were polished to a  $0.3\ \mu\text{m}$  finish, carbon coated, and analyzed using a JEOL 8530F microprobe at NASA's JSC. All analyses were conducted using an accelerating voltage of 15 keV and a beam current of 15 nA. A  $5\ \mu\text{m}$  spot size was employed for all analyses. Elements analyzed include Si (Springwater olivine used as a standard), Mg (San Carlos olivine), Al (VG-2 glass), Ca (Sitkin-Anorthite), and Fe (San Carlos olivine).

**VNIRS Analyses.** Reflectance spectra were acquired under ambient laboratory conditions at Johnson Space Center using an Analytical Spectral Devices (ASD) FieldSpec-3 VNIR spectrometer ( $0.35$  to  $2.50\ \mu\text{m}$ ) configured with a reflectance probe that contains its own light source. Spectra were collected relative to a Spectralon diffuse reflectance standard (99%) and converted to absolute reflectance by instrument software. Each spectrum is the average of 50 wavelength scans.

**Results: XRD Analyses.** The natural San Carlos olivine that was crushed and analyzed by XRD provided a 100% semi-quantitative match to  $\text{Fe}_{0.188}\text{Mg}_{1.812}\text{O}_4$ , consistent with San Carlos olivine which has an Mg# of 91. All forsterite samples analyzed by XRD produced patterns consistent with a 100% semi-quantitative match to the referenced forsterite in the XRD database, despite minor amounts of FeO being present. The single fayalite synthesis resulted in an XRD pattern consistent with the fayalite reference pattern.

**EPMA Analyses.** All results of EPMA analyses are given in Table 2. Sample F-S-003 did not have detectable FeO, which we attribute to it being synthesized in an alumina crucible. All other forsteritic samples were synthesized in a  $\text{Pt}_{95}\text{Au}_5$  crucible, which likely resulted in minor Fe contamination in the run products they hosted. We were able to synthesize forsteritic olivine with Mg# of 99.44, 99.63, 99.94, and 100 (assuming all Fe as ferrous).

**VNIRS Analyses.** Initial results from the VNIRS data are shown in Figure 1. Similar to the EPMA data, sample F-S-003, which had undetectable FeO by EPMA, also does not have a distinguishable  $1\text{-}\mu\text{m}$  absorption band. With increasing FeO content determined by EPMA, we see an increase in the depth of the  $1\text{-}\mu\text{m}$  absorption band from VNIRS.

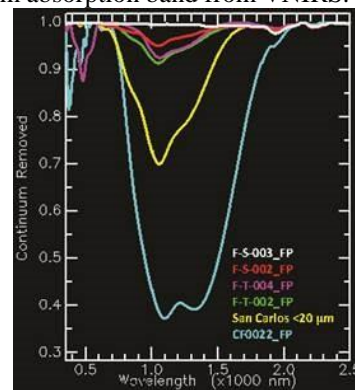


**Figure 1.** VNIRS spectra for all forsterite samples. FP = Fine Powder

**Discussion:** Although our preliminary results have considered only small variations across the olivine solid-solution series from  $\text{Fo}_{99.44}$  to  $\text{Fo}_{100}$ , we can see the presence of a  $1\text{-}\mu\text{m}$  absorption band with as little as 0.06 wt% FeO (i.e.,  $\text{Fo}_{99.94}$ ). We plan to analyze our run products by Mossbauer spectroscopy to determine more accurate Mg#'s for each of our synthetic olivine powders. Establishment of accurate Mg#'s will be important for placing constraints on how the band depth of a  $1\text{-}\mu\text{m}$  absorption feature changes as a function of  $X_{\text{FeO}}$  in olivine. Future work will involve synthesis and characterization of olivine with FeO abundances between  $\text{Fo}_{99.94}$  and  $\text{Fo}_{100}$ . In addition, we will synthesize and characterize various Mg-rich pyroxene compositions for better applicability to low-FeO planetary bodies.

**References:** [1] Burns, R.G., (1993), New York: Cambridge University Press. 551. [2] Klima, R.L., et al. (2007) *Meteoritics & Planetary Science*. **42**(2): p. 235-253. [3] Nittler, L.R., et al., (2011) *Science*. **333**(6051): p. 1847-1850. [4] Pieters, C.M., (1986) *Reviews of Geophysics and Space Physics*, 1986. **24**: p. 557-578. [5] Zellner, B., et al., (1977) *Geochimica et Cosmochimica Acta*, 1977. **41**: p. 1759-1767. [6] Dyar, M.D., et al., (2009) *American Mineralogist*, 2009. **94**(7): p. 883-898.